LA-UR- 97-2360

Approved for public release; distribution is unlimited.

Title: MODELING AND ANALYSIS OF THE HIGH ENERGY LINER EXPERIMENT, HEL-1

CONF-9706113--14

Author(s): RICKEY J. FAEHL, XPA, B259
PETER T. SHEEHEY, XPA, B259
ROBERT E. REINOVSKY, DX-DO, F672
IRVIN R. LINDEMUTH, XPA, B259
VNIEEF
A. M. BUYKO
V. K. CHERNYSHEV
S. F. GARANIN
V. N. MOKHOW
V. B. YAKUBOV

Submitted to: 11TH IEEE INTERNATIONAL PULSED POWER CONFERENCE

JUNE 29 - JULY 2, 1997
Baltimore, MD

MASTER

DISCLAIMER

Los Alamos
NATIONAL LABORATORY

DISTRIBUTION OF THIS DOCUMENT IS UNLIMITED

MODELING AND ANALYSIS OF THE HIGH ENERGY LINER EXPERIMENT, HEL-1

R. J. Faehl, P. T.Sheehey, R. E. Reinovsky, and I. R. Lindemuth
Plasma Applications Group and Pulsed Power ProgramOffice,
Los Alamos National Laboratory, Los Alamos, New Mexico 87545.

A.M. Buyko, V. K. Chernyshev, S. F. Garanin, V. N. Mokhov, and V. B. Yakubov,
All-Russia Scientific Institute of Experimental Physics, 607200,Sarov (Arzamas-16),
N. Novgorod Region, Russia

A high energy, massive liner experiment, driven by an explosive flux compressor generator, was conducted at VNIIEF firing point, Sarov, on August 22, 1996. We report results of numerical modeling and analysis we have performed on the solid liner dynamics of this 4.0 millimeter thick aluminum liner as it was imploded from an initial inner radius of 236 mm onto a Central Measuring Unit (CMU), radius 55 mm. Both one- and two-dimensional MHD calculations have been performed, with emphasis on studies of Rayleigh-Talylor instability in the presence of strength and on liner/glide plane interactions.

One-dimensional MHD calculations using the experimental current profile confirm that a peak generator current of 100-105 MA yields radial liner dynamics which are consistent with both glide plane and CMU impact diagnostics. These calculations indicate that the liner reached velocities of 6.9-7.5 km/s before CMU impact. Kinetic energy of the liner, integrated across its radial cross-section, is between 18-22 MJ. Since the initial goal was to accelerate the liner to at least 20 MJ, these calculations are consistent with overall success.

Two-dimensional MHD calculations were employed for more detailed comparisons with the measured data set. The complete data set consisted of over 250 separate probe traces. From these data and from their correlation with the MHD calculations, we can conclude that the liner deviated from simple cylindrical shape during its implosion. Two-dimensional calculations have clarified our understanding of the mechanisms responsible for these deformations. Many calculations with initial outer edge perturbations have been performed to assess the role of Rayleigh-Taylor instability. Perturbation wavelengths between 4-32 mm and amplitudes between 8-240 μm have been simulated with the experimental current profiles. When strength is omitted short wavelengths are observed to grow to significant levels; material strength stabilizes such modes in the calculations. Wavelengths long compared to the liner thickness grow to large amplitude in either case. Calculations which include the glide planes (electrodes) exhibit less mode growth than quasi-infinite ones. Mass thinning of the liner results in greater acceleration near the glide planes than near the midplane. The overall liner shape which results is strongly bowed, with a smooth ellipsoidal inner surface.

Introduction

LANL and VNIIEF conducted a joint experiment which used an extremely energetic explosive generator to implode a massive, solid aluminum liner on August 22, 1996. A set of five large, one meter diameter, explosive disk generator modules (DEMG) were employed to accelerate a 4 mm thick, 10 mm long liner onto a Central Measuring Unit (CMU) target. The CMU, centered on the axis with a radius of 55 mm, contained an array of optical pins, contact pins, piezoelectric probes, and B-dot probes. This DEMG configuration had demonstrated the capability to deliver 170 MA into a static, inductive load in a preliminary test. With the dynamic, imploding load, peak currents of 100-140 MA were anticipated, depending on performance of the seed current generator. The measured current peaked at 100-105 MA. Under these conditions, we infer that the liner kinetic energy was 20 ± 2 MJ when it impacted the CMU. This experiment reached unprecedented levels of peak current to a liner load, kinetic energy imparted to a liner, and

quantity of diagnostic data. It has placed a data point far out on edge of the imploding liner performance graph.

The primary objective of this experiment was to demonstrate that a solid liner could be electromagnetically accelerated to at least 20 MJ kinetic energy and imploded onto a target in a controllable fashion. Because of the extreme pulsed power conditions, extensive diagnostics were implemented. Generator and transmission line diagnostics included B-dot probes, voltage probes, Rogowski coils, and a Faraday rotation optical sensor. These are discussed in detail in other papers[1-3]. Probes were also set into the surface of the glide planes (electrodes) to directly measure the arrival times of the liner at various radii. The glide plane probes included B-dot probes, piezoelectric probes, and optical beam interruption sensors. Finally, a large array of optical, contact, and piezoelectric pins were placed above, flush, or recessed into the surface of the CMU to measure the liner shape as it impacted the target. One-dimensional MHD calculations were used to estimate the radial location of the liner as a function of time, its radial velocity distribution, and the fraction of the liner mass which was not melted. These calculations have proved to be very useful for establishing scaling trends. For detailed comparisons with the diagnostics we have employed two-dimensional calculations, which are able to follow the liner deformation throughout the current pulse. The latter include both Lagrangian and Eulerian simulations, with both strength and realistic resistivities. The one-dimensional ones are Lagrangian calculations. The Eulerian calculations are the only two-dimensional simulations with full MHD treatment.

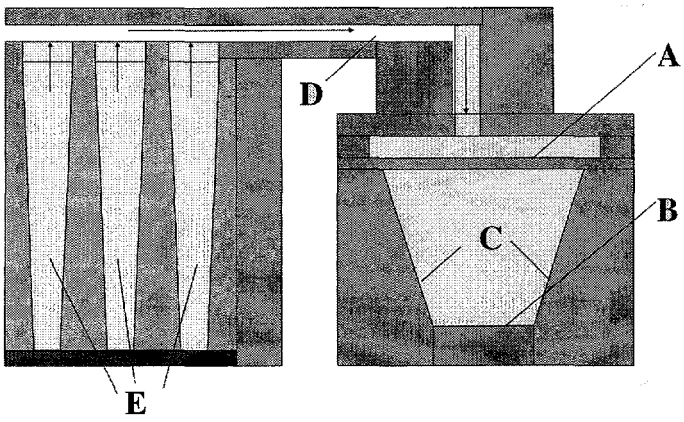

Figure 1. Experimental configuration for HEL-1: (A) Aluminum Amg-6 alloy liner, (B) central measuring unit (CMU), (C) steel electrodes/glidesplanes, (D) power flow channel, (E) disk electromagnetic generator (DEMC) modules.

The experimental configuration showing the initial liner position, the glide planes, and CMU is shown in Figure 1. The inner radius of the liner was 236 mm and its thickness, 4.0 mm. It was fabricated from aluminum alloy AMg-6, which has a yield strength of 15 kg/mm^2 and a density of 2.64 g/cm^3. The glide planes were made of steel, with a pitch angle of 6^o with respect to vertical. The two glide planes were separated by approximately 100 mm at the top. This was therefore the effective liner length. The glide plane separation at the CMU narrowed down to 62 mm. The CMU was segmented into a LANL diagnostic section and a VNIIEF one, the division occurring at the midplane.

One-dimensional MHD calculations and comparisons with data

LANL and VNIIEF independently performed one-dimensional MHD calculations of the liner implosion, using the measured current pulse. Measurements using a variety of magnetic and optical diagnostics yielded a peak current of between 100-105 MA. A typical measurement, from a B-dot probe, shown in Figure 2, corresponds to 104 MA. Individual measurements varied by

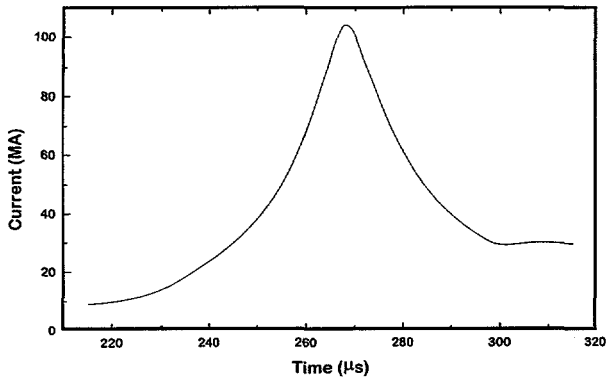

Figure 2. Typical experimental current pulse, starting with onset of DEMG operation; I_{max} = 104 MA.

no more than a few percent, and the pulse shape was consistently the same. It should be noted that all time measurements have been correlated to a common time base. The 'seed current' generator was initiated at time, t_o. On this time scale, the DEMG was initiated at t = 215.8 μs. CMU impact occurred in the time range t = 294.2-296.3 μs. There are reasons to believe that this range of impact times is related to the liner shape, not measurement uncertainties.

As a consistency check, one-dimensional MHD calculations with the measured current pulse shape were performed, with peak current varied between 95-109 MA. The radius of the inner liner edge as a function of time is shown in Figure 3 for four currents, I = 94.9, 99.4, 103.8, 108.4 MA. These curves are compared with data, especially the set of impact times onto the CMU. The curve corresponding to a peak current of 94.9 MA yields an impact time outside the credible timing range (t_{impact} > 301 μs). Likewise, the curve for 108.4 MA gives an impact time of t_{impact} = 294.1 μs. While there is CMU impact near this time, impact near the midplane where the one-dimensional calculations should be most valid is over 2 μs later. The curves for peak currents of 99.4 and 103.8 MA give impact times of 298.9 and 296.1 μs. On the basis of these one-dimensional calculations, we would infer that a peak current of 103.8 MA is close to the proper experimental figure. The lower current with its delayed impact time is outside the range of impact times, but a difference of 2.5 μs out of a total implosion time of over 80 μs is regarded as too small to be a conclusive calculational measure. Quantitative comparisons require correlation to a fuller fraction of the data set with two-dimensional calculations.

To complete the summary of the one-dimensional calculations, the peak velocity computed at 104 MA reached 7.5 km/s, while that for 99.4 MA reached 6.9 km/s. Total kinetic energy for the two currents was 22 and 18 MJ respectively. An important quantity for assessing stability of the liner is the amount of the material still in an elastic-plastic, strength-retaining state at impact. We estimate that between 50-65% of the aluminum mass was still under strength at the time of CMU impact on the basis of the one-dimensional simulations.

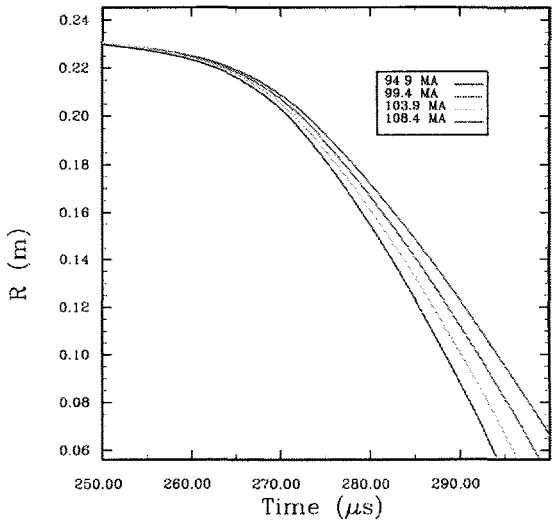

Figure 3. Radius of inner edge of liner profile versus time for I_{max}= 94.9, 99.4, 103.8, 108.4 MA, (1-D MHD).

Two-dimensional MHD calculations and stability

At the outset of this project, there was considerable uncertainty about the effect of Magnetic Rayleigh-Taylor on liner performance. Destruction of liner integrity by such a process would severely limit imploding liner applications at high energies. The one-dimensional calculations indicated that a large fraction of the liner material would remain in an elastic-plastic state. Strength in this state was felt to be a stabilizing factor. A number of studies have shown that even solid liners can be susceptible to acceleration instabilities, however.[4-7] Two-dimensional MHD calculations using the experimental parameters were conducted to address this question more concretely.

Calculations were set up with an initial perturbation 'machined' into the outer edge of the liner, $r_{out} = r_o + A\sin(2\pi z/\lambda_o)$. Reflecting boundary conditions were employed in the axial direction to avoid complications arising from glide plane interactions. The liner inner radius was taken to be 236 mm and its thickness, d = 4.0 mm, consistent with the experiment. The sinusoidal amplitude, A, was varied between 10-400 μm and wavelengths between 4-32 mm. A significant source of uncertainty was the strength properties of the aluminum alloy AMg-6. Its normal yield strength is known to be 15 kg/mm^2, its ultimate strength, 35 kg/mm^2. (For the alloy 1100-0, these numbers are 3.5 and 9.0 kg/mm^2, respectively.) Previous studies[4-5] indicated that stability is better correlated with ultimate yield strength. Data for AMg-6 in the expected pressure regimes is questionable. There is also uncertainty about the conductivity scaling of this alloy for expected conditions. These unknowns limit the quantitative value our calculations.

There are indications that a finite amplitude threshold exists[5-7] for the stability of solid liners. Thickness variation measurements were taken for the fabricated liner. These measurements showed that thickness did not vary by more than 17 μm. The first calculation was performed with A = 400 μm and λ = 8 mm. This calculation conclusively demonstrated that gross perturbations overwhelm any stabilizing effects due to material strength. Figure 4 shows that the liner is on the verge of being destroyed after imploding to a radius of only 200 mm. On the other hand, when the amplitude was reduced to 10 μm, corresponding to a peak-to-peak variation of 20 μm, the liner reached the radius of the CMU with only minor deformation. These calculations indicate the actual liner, with thickness varying by no more than 17 μm, should not be ruptured before it implodes onto the target CMU.

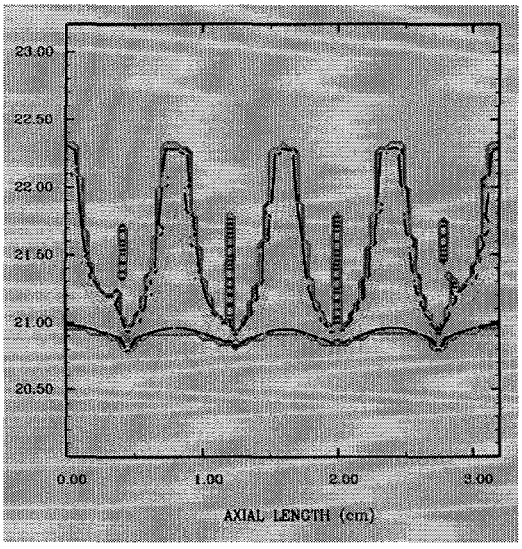

Figure 4. Density contours for typical 2-D MHD calculation with initial perturbations on outer edge; A = 240 μs, λ = 8 mm.

Because of our uncertainty about the pressure scaling of material strength for AMg-6, we conducted a series of simulations in which the strength parameters were varied parametrically. These showed that even short

wavelength perturbations ($\lambda < 4$ mm = d) grew to significant levels when material strength was reduced to small values. Longer wavelengths also grew in the "weak" material. When strength was progressively increased, less growth was noted at short wavelengths. Growth for wavelengths longer than d, the liner thickness, is less strongly effected than for shorter ones.

Two-dimensional MHD calculations, including glide planes

The experimental configuration includes slanted electrodes (c.f. Figure 1). The glide plane angle for this experiment was 6°. Since this liner must shear at the glide plane corners, and then be continuously scraped off by the glide planes, we anticipated that the liner/glide plane interaction would have significant effects on the liner dynamics. Two-dimensional MHD calculations were performed to quantify the magnitude of such effects.

One of the first issues addressed in these calculations was the shearing of the liner at the glide plane corners. To focus on this issue, a sharp corner was simulated, instead of the stepped corner used in the experiment. It was found that full current pulse shape, including that of the seed current generator, was required. Even though the liner did not actually shear until 20-30 μs after the onset of the DEMG, the effect of the seed current, which reached over 9 MA, resulted in a 3-4 mm bow in the center of liner. The liner was thus placed in tension even before the material along the glide plane began to move. After the magnetic pressure became great enough to shear the corner, the full liner was accelerated inward. After a radial travel of 80 mm, the material adjacent to the glide plane had actually caught up with the center. This quasi-flat state was transient, however. Mass thinning of the liner near the glide planes resulted in higher acceleration in this region than in the center. For radii less than 160 mm, the liner became progressively bowed inward.

Figure 5 shows a typical calculated mass distribution shortly before CMU impact. The peak current used in this calculation was 99.4 MA. Material near the glide plane has run significantly ahead of mass near the center. It is approximately 15 mm ahead by this late time. The liner velocity on the inner surface near the center plane was 7.5 km/s at this time. Velocities increased nearer the glide planes, but peak velocities greater than 7.6 km/s??? are not observed. Such velocities are not consistent with one-dimensional calculations, in which peak inner surface velocities did not reach 7.0 km/s for a peak current of 99.4 MA. We have not fully resolved this point at present, but suspect it is related to decreasing accelerated mass as the liner propagates down the slanted glide planes.

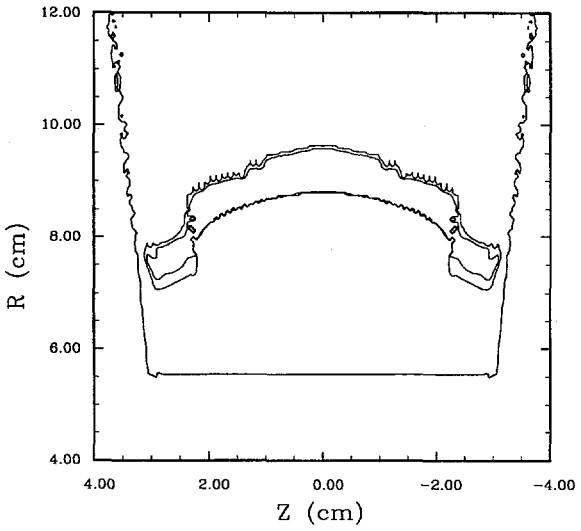

Figure 5. Density contours for a liner/glide plane 2-D MHD calculation near impact with CMU; I_{max} = 99.4 MA.

Once the liner shears at the glide plane corners, the region adjacent to the glide plane is always in a liquid, strengthless state. Details of this transition are being studied in laboratory

experiments[8]. In the calculations, interaction of this liquid layer with the bulk solid state of the liner leads to mass thinning near the glide plane. Figure 6 shows the boundary between solid and liquid material for the configuration in Figure 5. It is possible that this effect is exaggerated in the calculations compared with the experimental configuration. Preliminary results from PEGASUS II experiments[8] support this suggestion. The overall shape of the liner is probably similar to Figure 5, however. Reduced mass near the liner leads to enhanced acceleration, enhanced magnetic field penetration, and more joule heating. In support of this hypothesis, both VNIIEF and LANL B-dot probes located just above the CMU detect a significant field penetration through the liner at a time of 5-10 μs before bulk mass impact. This range is exactly where the calculations indicate that appreciable flux injection interior to the liner occurs. Several MA's of current apparently circulate between the CMU and the inner liner surface during this final phase of the implosion.

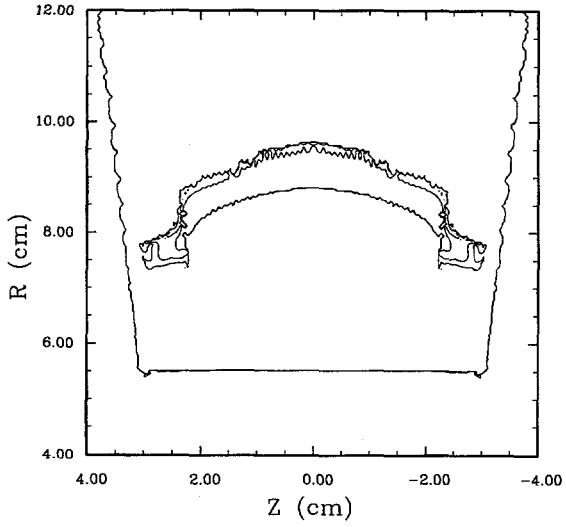

Figure 6. Melt Contours for the density distribution shown in Figure 5.

A variety of probes were imbedded in the glide plane, at several azimuths and at radii of 130.8 and 105.8 mm. The most straightforward signals to compare with the calculations were, inductive probes and piezoelectric probes, which measured pressure. The latter presumably measured the arrival of the inner surface of the liner. The B-dot probes were intended to measure the arrival of the outer liner surface, assuming negligible field penetration. The MHD calculations showed significant field penetration in the hot, liquid material near the glide planes. Regardless of correlations with the liner surfaces, an analogous signal can be constructed from the calculational results, and these can be directly compared to the measured signals. The most accurate piezoelectric probes yielded arrival times of 284.2 and 288.2 μs. Typical calculations gave pressure signals commencing at 283.4 and 287.4 μs. Similarly, the initiation of inductive signals on the B-dot probes occurred at 284 and 287 μs. In the calculations, the corresponding times were 283.6 μs and 287.4 μs. Discrepancies of less than one μs in arrival times are felt to be very good agreement for these conditions.

Finally, LANL fielded a series of optical pins, which protruded from the CMU. According to expectations, these pins should not have yielded significant signals until impacted by pressures of at least 0.5 Mbar(50 Gpa). Some of the pins behaved as expected. A particularly clean set of signals was obtained from a series of pins which extended 10 mm above the CMU along the same azimuth. Their axial positions, measured from the midplane, were at z = 5, 15, 20, 25 mm. These pins gave sharp risetimes at 296.25, 295.00, 294.60, and 294.22 μs, respectively. The calculated arrival times at the tips of such pins were 295.0, 294.4, 293.1, and 292.4 μs for the configuration shown in Figs 5 and 6. The overall agreement is felt to be excellent between calculation and measurement. Taken together, the agreement provides strong evidence that the actual liner shape was similar to that depicted in Figs. 5 and 6.

Conclusions

The high energy liner experiment conducted jointly by VNIIEF and LANL demonstrated that currents of 100-105 MA could be used to implode of solid liner onto a target. Correlation of data with calculations indicates that the liner deformed smoothly during the course of the implosion. It probably did not rupture. Further study is required to fully understand all the ramifications of the data, but the experiment did establish the feasibility of liner implosions at such extremely high currents.

References

1. V.K.Chernyshev, V.N.Mokhov, et al, "Study of Condensed High-Energy Liner Compression in HEL-1 Experiment", Proc.11th IEEE Pulsed Power Conference, (1997).
2. R.E.Reinovsky, et al, "HEL-1: A DEMG Based Demonstration of Solid Liner Implosions at 100 MA" , Proc.11th IEEE Pulsed Power Conference,(1997).
3. David A. Clark, B.G. Anderson, et al, "High Energy Imploding LinerExperiment HEL-1: Experimental Results", Proc.11th IEEE Pulsed Power Conference, (1997).
4. J.F. Barnes, P.J. Blewett, R.G. McQueen, K.A. Meyer, and D. Venable, "Taylor Instability in Solids," J. Appl. Phys. **48**, (1974), 727.
5. J.F. Barnes, D.H. Janney, R.K. London, K.A. Meyer, and D.H. Sharp, "Further experimentation on Taylor Instability in solids," J. Appl. Phys. **51**, (1980), 4678.
6. D.C. Drucker, "A Further Look at Rayleigh-Taylor and other Surface Instabilities in Solids," Ingeneur-Archiv **49**, (1980), 361.
7. J.W. Swegle and A.C. Robinson, "Acceleration instability in elastic-plastic solids. I. Numerical simulations of plate acceleration," J. Appl. Phys. **66**, (1989), 2838; A.C. Robinson and J.W. Swegle, "Acceleration instability in elastic-plastic solids, II. Analytical techniques,"J. Appl. Phys. **66**, (1989), 2859.
8. W.L.Atchison, et. Al, "Evaluation of Magneto Rayleigh-Taylor Mode Growth using Comparisons of 2D Calculations with Radiography," Proc. 11th IEEE Pulsed Power Conference, (1997).